Journal of Solid State Chemistry **150,** 336–341 (2000)
doi:10.1006/jssc.1999.8599, available online at http://www.idealibrary.com on IDEAL®

Uranium's Valency in U_3S_5

H. Kohlmann[1] and H. P. Beck

Institut für Anorganische und Analytische Chemie und Radiochemie, Universität des Saarlandes, Postfach 15 11 50, D-66041 Saarbrücken, Germany

Received October 1, 1999; in revised form November 19, 1999; accepted December 4, 1999

U_3S_5 has been prepared by chemical transport reaction and investigated using X-ray powder diffraction, FTIR spectroscopy, electrical resistivity measurements, and X-ray photoelectron spectroscopy. U_3S_5 is a semiconductor with a thermal band gap $E_g = 78.1(4)$ meV (298 K $< T <$ 50 K), which closes gradually to 3.4(4) meV for $T < 25$ K. Photoelectron spectroscopy on single crystals of U_3S_5 and β-US_2 suggest a mixed valency of uranium in U_3S_5. Physical and structural data are consistent with a mixed-valent model $(U^{3+})_2U^{4+}(S^{2-})_5$. A brief survey of literature data on crystal structure and physical properties of uranium sulfides and selenides is given. © 2000 Academic Press

Key Words: **uranium chalcogenides; mixed valency; photoelectron spectroscopy.**

1. INTRODUCTION

One of the most interesting topics in the solid state chemistry of uranium chalcogenides is the valency of uranium. Following the general trend for transition elements (1, 2) high oxidation states of uranium as in oxides are not achieved in sulfides and selenides. Here the maximum valency is +4 with the electron configuration [Rn]$5f^2$. Hence, the key question in view of the physical properties of these materials is whether the at least two remaining f electrons are itinerant or localized at the uranium ion.

The triuranium pentasulfide U_3S_5 is of special interest because it is at the borderline between the metallic uranium rich compounds and the semiconducting chalcogen-rich compounds. The crystal structure data led to the assumption of a mixed-valency model with U(III) and U(IV) in the ration 2:1, according to the formula $(U^{3+})_2U^{4+}(S^{2-})_5$ (3). This has been derived from a qualitative analysis of the U–S distances. On the other hand the calculated interatomic distances are rather inaccurate, as precise lattice parameters are lacking. Clues for the mixed-valency model could also be derived from magnetic data (4); however, these data cannot give direct evidence. XPS spectra gave only single lines for uranium core levels (5), whereas for the mixed valency model splitting of lines is expected. Reports on the electrical conductivity are controversial (6, 7).

In view of these inconsistencies we decided to reinvestigate the structural and physical properties of U_3S_5. Special attention has been paid to the preparation of pure material and the growth of single crystals suitable for physical measurements. For a comparison, β-US_2 single crystals have also been investigated. Recently, a detailed study on the transport properties of U_3S_5 was published (8); the present work was carried out independently from the former.

2. EXPERIMENTAL DETAILS

2.1. Synthesis

Black, shiny single crystals of U_3S_5 and β-US_2 were grown by chemical transport in evacuated sealed silica tubes using iodine as a transport agent (0.2–0.5 mg I_2/cm^3 ampoule volume, ampoules with outer diameter 16 mm and wall thickness 1.5 mm) with temperature gradients $T_2 =$ 1190 and 1070 K, $T_1 = 1100$ and 870 K for U_3S_5 and β-US_2, respectively. Crystals up to three millimeters in length grew in the colder zone. For the synthesis of β-US_2, stoichiometric mixtures of the elements were used (uranium ingot, Kristallhandel Kelpin, 99.9%, ^{235}U content 0.0361%; sulfur, Riedel de Haën, 99.5%, purified by sublimation prior to use). For the synthesis of U_3S_5, mixtures of the elements substoichiometric with regard to sulfur ($n_{(S)}/n_{(U)} = 1.5$ instead of 5/3) were used, in order to prevent the formation of α-US_2 as a by-product (see the discussion in Section 3.1). The residual in the hotter zone at T_2 consisted of UOS and Si. Minor amounts of UOS as a by-product of U_3S_5 were also found in the colder zone at T_1. Single crystals of U_3S_5 have a characteristic prismatic habitus and could be easily distinguished from crystals of the by-product UOS, which always formed nearly isometric quadratic bipyramids with both the top and bottom corners truncated. All handlings were carried out in an argon-filled glove box.

[1] To whom correspondence should be addressed. Present address: Laboratorie de Cristallographie, Quai Ernest Ansermet 24, CH-1211 Genève 4, Switzerland. E-mail: Holger.Kohlmann@cryst.unige.ch.

0022-4596/00 $35.00

2.2. X-Ray Diffraction

As reliable structural data for U_3S_5 are already available (3) and our single-crystal studies on a precession camera confirmed these results, no refinement of the crystal structure was performed in this work. In view of the low accuracy of the lattice parameters derived from single-crystal data (3), we have redetermined them from X-ray powder diffraction data. They were taken on a capillary sample (0.1 mm inner diameter, Si as internal standard) on a four-circle powder diffractometer with a position sensitive detector oriented in the ω-2Θ plane (Cu$K\alpha_1$ radiation). Lattice parameters have been refined to the values $a = 1175.19(3)$, $b = 810.21(2)$, $c = 742.05(2)$ pm using the computer program DBWS-9411 (9). Interatomic distances have been calculated using the lattice parameters refined in this work and the positional parameters given in Ref. (3).

Low-temperature X-ray diffraction data down to $T = 10$ K were collected on a Huber–Guinier diffractometer G645 (Cu$K\alpha_1$ radiation). No structural phase transition was observed.

2.2. Electrical Resistivity

DC resistivity was measured using the standard four-probe technique on an aggregate of intergrown crystals ($0.5 \times 2 \times 3$ mm^3) using platinum wires contacted with indium from room temperature down to 15 K and back to room temperature in increments of 2 K. The data are shown in Fig. 1 as a $\log\rho$ vs $1/T$ plot. The room temperature resistivity is 94 mΩ cm.

2.3. FTIR Spectroscopy

IR spectra of a powder sample of U_3S_5 were recorded with an FT-IR spectrometer (Perkin–Elmer, system 2000 FT-IR) in diffuse reflection in the range $10800 > \hat{\nu} > 370$ cm^{-1}.

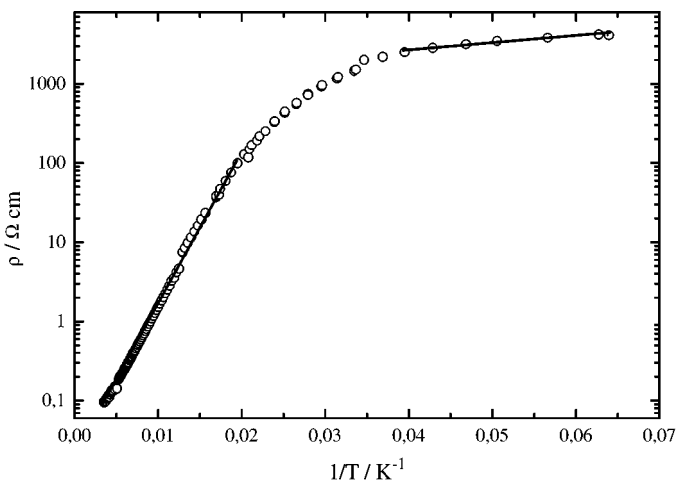

FIG. 1. Electrical resistivity of U_3S_5 as a function of $1/T$.

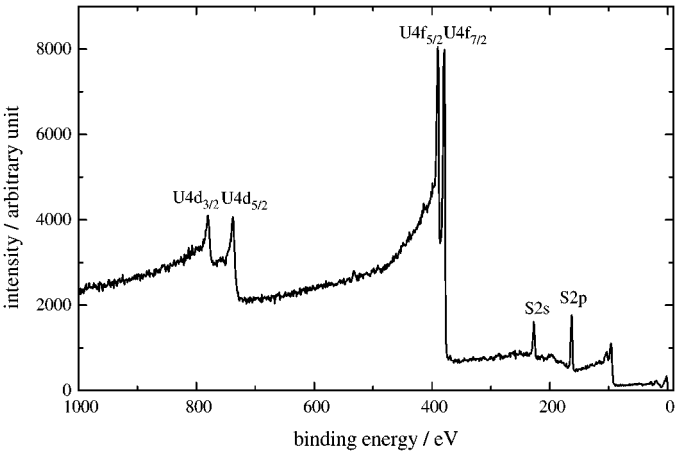

FIG. 2. X-ray photoelectron spectra of U_3S_5.

2.4. X-Ray Photoelectron Spectroscopy (XPS)

A single crystal of U_3S_5 of the size $3 \times 2 \times 2$ mm^3 has been used for XPS measurements at room temperature. It was transferred from an argon-filled glove box to the spectrometer in a transport vessel for air-sensitive compounds. Since photoelectron spectroscopy is a surface-sensitive method, scraping with a diamond file and XPS measurements were carried out under ultra high vacuum conditions ($p < 10^{-7}$ Pa). Contamination with oxygen and carbon could be avoided using this procedure, as proven by the absence of O1s and C1s core levels. XPS data were collected with an SSI M-Probe Small Spot Spectrometer with monochromatic Al$K\alpha$ radiation ($\hbar\omega = 1486.6$ eV) and a focus on the sample of 300 µm. The spectrometer resolution was 0.8 eV. The position of the Fermi energy E_F was determined using a clean gold sample. No charging was observed for the U_3S_5 sample. Overview spectra were recorded with a step size of 1 eV; for a more detailed investigation, spectra of several core levels were recorded with a step size of 0.05 eV (Figs. 2 and 3).

3. RESULTS AND DISCUSSION

3.1. Chemical Transport of U_3S_5 and US_2

Chemical transport of U_3S_5 starting from stoichiometric mixtures of the elements always led to a product that contained considerable amounts of α-US_2. This is caused by the reactivity of U_3S_5 toward silica at higher temperatures as formulated in

$$6U_3S_5 + 3SiO_2 \rightarrow 6UOS + 12US_2 + 3Si. \qquad [1]$$

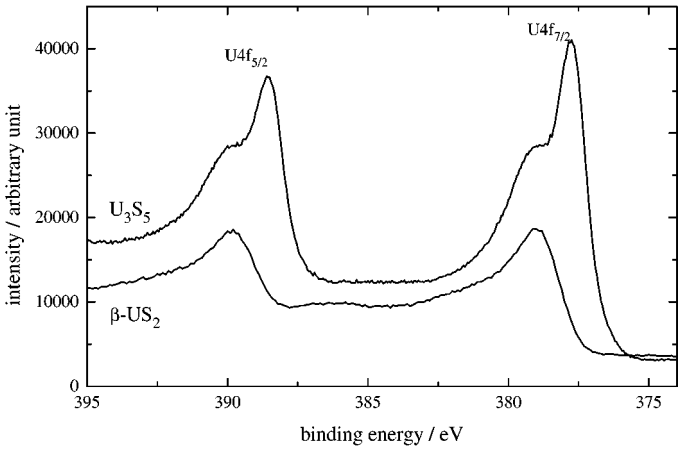

FIG. 3. U4*f* core-level spectra of U_3S_5 (above) and β-US_2 (below).

Because of the lower reactivity of US_2 toward silica, only neglegible amounts of UOS are found in the β-US_2 samples.

In view of this problem, the use of a mixture of uranium and sulfur with a stoichiometric ratio 2:3 instead of 3:5 is advantageous for the preparation of U_3S_5. However, the formation of UOS and Si is unavoidable under these conditions. Fortunately, the transportation rate of UOS was found to be very low under these experimental conditions compared to that of U_3S_5, and for Si no transport was observed. Hence, the major part of these by-products remains in the hot zone at T_2, and they are well seperated from the reaction product at T_1.

The difference in the transportation rates of U_3S_5 and UOS can be explained by a thermodynamical analysis of the chemical transport reaction. Investigations of the chemical transport of uranium sulfides (10–15) have shown that these phases are probably transported by gaseous uranium triiodide according to

$$2U_3S_{5(s)} + 9I_{2(g)} \underset{T_1}{\overset{T_2}{\rightleftarrows}} 6UI_{3(g)} + 5S_{2(g)} \qquad [2]$$

$$2US_{2(s)} + 3I_{2(g)} \underset{T_1}{\overset{T_2}{\rightleftarrows}} 2UI_{3(g)} + 2S_{2(g)} \qquad [3]$$

$$2UOS_{(s)} + 3I_{2(g)} \underset{T_1}{\overset{T_2}{\rightleftarrows}} 2UI_{3(g)} + S_{2(g)} + O_{2(g)}. \qquad [4]$$

The free enthalpy of reaction [4] is roughly estimated to be $\Delta_r G_{[4]}^{1200K} = 676$ kJ/mol from thermodynamical data of uranium compounds and sulfur (16–18). For reaction [3] Smith and Cathey derived a free reaction enthalpy $\Delta_r G_{[3]}^{1200K} = 42$ kJ/mol (10). The rule that an effective chemical transport requires a free transport reaction enthalpy close to zero (19) is obviously much better fulfilled for the chemical transport of US_2 (Eq. [3]) than for UOS (Eq. [4]). Unfortunately, no such estimation can be made for reaction [2], since thermodynamical data on U_3S_5 are lacking. However, it can be concluded that the reaction enthalpies of reactions [2] and [3] are of the same order, because both U_3S_5 and US_2 are transported under the same conditions with nearly identical rates. Thus, on a qualitative basis, the conclusions drawn for US_2 can be extended to U_3S_5. This finding from thermodynamical analysis is in agreement with the experiment. For the synthesis of U_3S_5 the product is tranported much faster (2 mg/h) than the by-product UOS, whose major part remains in the hot zone T_2. A further confirmation of this result is provided by experiments on the chemical transport of pure UOS, where the transportation rates did not exceed 0.15 mg/h, even under optimized conditions.

From the thermodynamical point of view, the high formation enthalpy of UOS causes its formation during the synthesis of U_3S_5, but this also makes it possible to separate it from the binary uranium sulfides by means of chemical transport reactions.

3.2. *Crystal Chemistry*

The lattice parameters of U_3S_5 determined here from X-ray powder diffraction data do not differ significantly from earlier results (3), but they are more precise. Calculated mean U–S distances are 293.0(1) pm for the uranium atom in the eight-fold position and 274.8(1) for the uranium atom in the four-fold position with ECoN values (20) of 7.9 and 6.9, respectively. These distances match well both with reference values for $d(U_{[8]}^{3+}\text{-}S) = 293$ pm and $d(U_{[7]}^{4+}\text{-}S) = 275$ pm (coordination number in brackets), as derived in a systematic study on the relation between uranium valency and distances (21) and with the sum of ionic radii (293 pm and 276 pm), which have been estimated for the appropriate coordination number from the data in (22).

3.3. *Electrical Transport Properties*

The temperature dependence of the electrical resistivity clearly shows the characteristics of a semiconductor (Fig. 1). From the slope of the linear parts of the $\log \rho$ vs $1/T$ plot the thermal band gap E_g has been calculated according to the formula for intrinsic semiconductors $\rho \sim e^{E_g/2kT}$. A band gap $E_g = 78.1(4)$ meV is found in the $298 < T < 50$ K temperature region. Below 50 K the band gap decreases graduallt to $E_g = 3.4(4)$ meV for $T < 25$ K. This closing of the band gap was also observed in a recent investigation and attributed to the ferromagnetic ordering at $T_C = 28$ K (8).

3.4. *Spectroscopical Characterization*

3.4.1. FTIR spectroscopy. The FTIR spectrum of U_3S_5 displayed a low reflectivity of 12–20% over the whole

investigated energy range ($0.046 \leq E \leq 1.34$ eV), i.e., no absorption edge due to a band gap could be detected within this range. Under the assumption of semiconducting properties we conclude that the optical band gap of U_3S_5 at room temperature is smaller than 46 meV.

3.4.2. XPS. The measured XPS range of U_3S_5 is shown in Fig. 2. The U4*f* core level spectra of U_3S_5 (Fig. 3) show peaks at binding energies of 388.5 and 377.8 eV for U4$f_{5/2}$ and U4$f_{7/2}$, respectively, and shoulders to the side of higher energy at 389.7 and 379.0 eV. The positions of the latter are close to those of the corresponding U4$f_{5/2}$ and U4$f_{7/2}$ peaks of β-US_2 (Fig. 3), which is considered to contain U^{4+} only (23). Binding energies of typical compounds with U^{3+} are for U4$f_{5/2}$ and U4$f_{7/2}$, respectively, 388.9 and 378.1 eV (UCl_3), 388.9 and 378.2 eV (UBr_3) (24); for typical compounds with U^{4+}, 390.9 and 380.0 eV (UCl_4), 390.7 and 379.7 eV (UBr_4) (24), 391 and 380 eV (UO_2) (25). These data

TABLE 1
Crystal Structures and Physical Properties of Binary Uranium Sulfides and Selenides

US:	NaCl type, $Fm\bar{3}m$, $a = 547.3(2)$ pm (29)[a,b]
	Metallic appearance (7, 30); golden yellow (31); U^{4+} derived from crystal structure (29); $U^{3.5+}$ derived from crystal chemical analysis (21); metallic conductivity (6, 32); Fermi edge in UPS (33); $5f^2$ configuration for U derived from neutron diffraction data (34)
U_2S_3:	Sb_2S_3 type, *Pbnm*, $a = 1039(2)$, $b = 1063(2)$, $c = 388(1)$ pm (29)[c]
	Metallic appearance (30); purple gray (6); U^{4+} derived from crystal structure (29); metallic conductivity (6, 7)
U_3S_5:	U_3Se_5 type, *Pnma*, $a = 1175.19(3)$, $b = 810.21(2)$, $c = 742.05(2)$ pm (3, this work)[d]
	Black (35, this work); mixed valency derived from crystal structure (3); semiconductor with $E_g = 0.0189$ eV ($40 < T < 100$ K), anomaly at $T = 20$ K (8); semiconductor with $E_g = 0.0781(4)$ eV ($50 < T < 98$ (this work); mixed valency of uranium derived from XPS (this work)
α-US_2:	$SrBr_2$ type, *P4/n* (36), $a = 1029.3(1)$, $c = 637.4(4)$ pm (37)[d,e]
	Grayish black (38); black (39); crystal structure suggests U^{4+}; semiconductor with $E_g = 0.0031$ eV ($30 < T < 300$ K) (8)
β-US_2:	$PbCl_2$ type, *Pnma*, $a = 711.39(3)$, $b = 412.05(3)$, $c = 848.03(3)$ pm (23)[d]
	Black (23, 39); U^{4+} derived from crystal structure (23); semiconductor with $E_g = 1.2$ eV (23); semiconductor with $E_g = 0.022$ eV (10); semiconductor with $E_g = 0.00121$ eV ($12 < T < 50$ K), above $T = 50$ K pseudo-semimetallic behaviour (8)
γ-US_2:	anti-Fe_2P type, $P\bar{6}2m$, $a = 724.73(4)$, $c = 407.04(2)$ pm (40,[d] 41[f])
	Black (7, 41); U^{4+} derived from crystal structure (41); $\sigma(T = 298\text{ K}) = 3.86 \times 10^3\ \Omega^{-1}\ \text{cm}^{-1}$ (42)[g]
U_2S_5:	Th_2S_5 type, *Pcnb*, $a = 749(1)$, $b = 749(1)$, $c = 993.1(7)$ pm (43)[c]
	Crystal structure and magnetic susceptibility suggests polysulfide with U^{4+} (43)
US_3:	$ZrSe_3$ type, $P2_1/m$, $a = 539$, $b = 389$, $c = 1822$ pm, $\beta = 99.5^\circ$ (35)[c]
	Black (35, 39); crystal structure suggests polysulfide with U^{4+}
USe:	NaCl type, $Fm\bar{3}m$, $a = 573.9$ pm (44)[a,h]
	Gray with golden lustre (45); $U^{3.36+}$ derived from crystal chemical analysis (21); semimetallic conductor (46); metallic conductivity (45); intermediate configuration between $5f^2$ (U^{4+}) and $5f^3$ (U^{3+}) (28)
U_3Se_4:	Th_3P_4 type, $I\bar{4}3d$, $a = 882.0(1)$ pm (47)[d]
	Gray (45); gray metallic appearance (42); $U^{3.3+}$ derived from crystal structure (47)[i]; $\sigma(T = 298\text{ K}) = 1.53 \times 10^3\ \Omega^{-1}\ \text{cm}^{-1}$ (42)[g]
U_2Se_3:	Sb_2S_3 type, *Pbnm*, $a = 1130$, $b = 1094$, $c = 406$ pm (48)[a]
	Gray (45); metallic conductivity (45); semimetallic conductor (46)
U_3Se_5:	U_3Se_5 type, *Pnma*, $a = 1243(2)$, $b = 848(1)$, $c = 777(1)$ pm (49)[d]
	Black (39, 50); mixed valency derived from crystal structure (49); semiconductor with $\rho(T = 298\text{ K}) = 0.2\ \Omega^{-1}\ \text{cm}^{-1}$ (51)
α-USe_2:	$SrBr_2$ type, *P4/n*, $a = 1070.0$, $c = 660.0$ pm (36)[d,e]
	U^{4+} derived from crystal structure (36); semiconductor (51)
β-USe_2:	$PbCl_2$ type, *Pnma*, $a = 745.5(2)$, $b = 423.20(5)$, $c = 896.4(2)$ pm (52)[d]
	Black (35, 39, 45); U^{4+} derived from crystal structure (52); semiconductor (51)
γ-USe_2:	anti-Fe_2P type, $P\bar{6}2m$, $a = 763.76(6)$, $c = 419.24(2)$ pm (41)[f]
	Black (45), dark gray (41), U^{4+} derived from crystal structure (41)
USe_3:	$ZrSe_3$ type, $P2_1/m$, $a = 565.2(2)$, $b = 405.6(3)$, $c = 1046.9(9)$ pm, $\beta = 115.03(6)^\circ$ (53)[d]
	Black (39, 53); crystal structure suggests polyselenide with U^{4+} (53); insulator (51)

[a] Powder diffraction, no crystal structure refinement.

[b] The phase transition to a rhombohedral distortion variant of the NaCl type at $P = 10$ GPa is considered to be correlated with a valency change from U^{3+} to U^{4+} (54).

[c] Single-crystal study, no crystal structure refinement.

[d] Crystal structure refinement on single-crystal data.

[e] The space group *P4/ncc* and a chalcogen deficiency had been claimed for α-US_2 and α-USe_2 (37) due to an unrecognized twinning (36). The correct space group is *P4/n* and both are stoichiometric compounds (36, 41)

[f] Rietveld refinement of the crystal structure.

[g] Probably low sample purity.

[h] Phase transition to CsCl type at $P = 20$ GPa without valency change of uranium (54).

[i] In Ref. (47), $U^{2.7+}$ was given mistakenly instead of $U^{3.3+}$.

suggest that the main peaks are the U4$f_{5/2}$ and U4$f_{7/2}$ signals of U^{3+} and the shoulders the corresponding signals of U^{4+}, thus confirming a mixed valency in U_3S_5.

3.5. Uranium's Valency in Binary Sulfides and Selenides

U_3S_5 is a semiconductor with a very small band gap ($E_g = 78.1(4)$ meV for $298 < T < 50$ K) which decreases at lower temperatures ($E_g = 3.4(4)$ meV for $T < 25$ K). XPS data on single crystals of U_3S_5 and β-US_2 suggest the presence of U^{3+} and U^{4+} in U_3S_5, and this is the first direct evidence for the mixed-valency of uranium in this compound. This finding is in full agreement with the interatomic distance calculations. Hence, the model of U_3S_5 as a mixed-valent, nonmetallic compound according to the formula $(U^{3+})_2\ U^{4+}\ (S^{2-})_5$ (3, 4) is confirmed. Mixed valency occurs also for neptunium in the isotypic Np_3S_5 and Np_3Se_5, as proven by ^{237}Np Mössbauer spectroscopy (26, 27).

To complete the picture, a brief survey of crystal structures and physical properties of binary uranium sulfides and selenides is given in Table 1. Emphasis is on those properties which shed some light on the question of the valency of uranium in these compounds. Magnetic data have not been included because they do not allow one to distinguish between U^{4+} and U^{3+} due to very close values of their magnetic moments. The valency +IV seems to be predominant in uranium sulfides and selenides in spite of the wide range of stoichiometries (Table 1). The uranium-rich sulfides US and U_2S_3 appear to be metallic. As a first approximation, using integer valencies, they can be described by the formulas $U^{4+}(e^-)_2S^{2-}$ (=US) and $(U^{4+})_2(e^-)_2(S^{2-})_3$ (=U_2S_3). In the second group, which contains the chalcogen-rich compounds, crystal structures and properties suggest that the three modifications of US_2 are ionic valence compounds $U^{4+}(S^{2-})_2$ and the chalcogen-rich phases are semiconductors and contain homonuclear chalcogen–chalcogen bonds according to the formulas $(U^{4+})_2(S^{2-})_3S_2^{2-}$ (=U_2S_5) and $U^{4+}S^{2-}S_2^{2-}$ (=US_3). The mixed-valent U_3S_5 is the only uranium sulfide with uranium in an oxidation state different from +IV. The uranium selenides show the same, but with a trend toward semimetallic behavior in the uranium-rich selenides compared to the metallic behavior of the corresponding sulfides. This reflects the expected increased covalency in selenides.

In general, 5*f* electrons of actinide compounds cannot be modeled correctly as purely itinerant or purely localized because of the vast expansion of the 5*f* shell (28), but especially for the semiconducting compounds a first approach with integer oxidation numbers seems to be reasonable. However, the limits of such simple models should always be kept in mind, especially in view of the small band gaps and the anomalies found in such compounds.

ACKNOWLEDGMENTS

We thank Dr. Rainer Zimmermann (Institute of Experimental Physics, University Saarbrücken, Germany) for the XPS measurements, Dr. R. Kremer (Max-Planck-Institute for Solid State Research, Stuttgart) for the measurement of the electrical conductivity, and Priv. Doz. Dr. Klaus Stöwe (Institute of Inorganic and Analytical Chemistry and Radiochemistry, University Saarbrücken, Germany) for the FTIR measurement. H. Kohlmann thanks the Federal State of Saarland (Germany) for a LGFG scholarship for doctoral research.

REFERENCES

1. J. B. Goodenough, *J. Alloys Compd.* **262–263,** 1 (1997).
2. J. Rouxel, *Adv. Synth. React. Solids* **2,** 27 (1994).
3. M. Potel, R. Brochu, J. Padiou, D. Grandjeau, and C. R. Sceances, *Acad. Sci. Series C* **275,** 1419 (1972).
4. H. Noël and J. Prigent, *Physica B* **102,** 372 (1980).
5. N. P. Sergushin, V. I. Nefedov, I. A. Rozanov, V. K. Slovyanskikh, and N. V. Gracheva, *Russ. J. Inorg. Chem. Engl. Transl.* **22,** 474 (1977).
6. A.N.L. 7279, *in* "Reactor Development Program Progress Report," Nov. 1966.
7. M. Picon and J. Flahaut, *Bull. Soc. Chim. France* 772 (1958).
8. L. Shlyk and R. Troc, *Physica B* **262,** 90 (1999).
9. R. A. Young, A. Sakthivel, T. S. Moss, and C. O. Paive-Santos, *J. Appl. Crystallogr.* **28,** 366 (1995).
10. P. K. Smith and L. Cathey, *J. Electrochem. Soc.* **114,** 973 (1967).
11. V. K. Slovyanskikh, G. V. Ellert, E. I. Yarembash, and M. D. Korsakova, *Inorg. Mater. Engl. Transl.* **2,** 827 (1966).
12. V. K. Slovyanskikh, G. V. Ellert, and E. I. Yarembash, *Inorg. Mater. Engl. Transl.* **3,** 1001 (1967).
13. V. K. Slovyanskikh, V. G. Sevast'yanov, and G. V. Ellert, *Russ. J. Inorg. Chem. Engl. Transl.* **15,** 1064 (1970).
14. V. G. Sevast'yanov, V. K. Slovyanskikh, and G. V. Ellert, *Russ. J. Inorg. Chem. Engl. Transl.* **16,** 1776 (1971).
15. V. G. Sevast'yanov, G. V. Ellert, and V. K. Slovyanskikh, *Russ. J. Inorg. Chem. Engl. Transl.* **17,** 7 (1972).
16. J. L. Settle and P. A. G. O'Hare, *J. Chem. Thermodynam.* **16,** 1175 (1984).
17. H. Wedemeyer, "Compounds of Uranium and Sulfur, Gmelin Handbook of Inorganic Chemistry," U Suppl. Vol. C10, 8th ed. Springer-Verlag, Berlin, 1984.
18. W. J. Moore and D. O. Hummel, "Physikalische Chemie," 3rd ed. de Gruyter, Berlin, 1983.
19. H. Schäfer, "Chemische Transportreaktionen." VCH, Weinheim, 1962.
20. R. Hoppe, *Z. Kristallogr.* **150,** 23 (1979).
21. H. Noël, *J. Solid State Chem.* **52,** 203 (1984).
22. R. D. Shannon, *Acta Crystallogr. Sect. A.* **32,** 751 (1976).
23. W. Suski, T. Gibinski, A. Wojakowski, and A. Czopnik, *Phys. Status Solidi A* **9,** 653 (1972).
24. E. Thibaut, J.-P. Boutique, J. J. Verbist, J.-C. Levet, and H. Noël, *J. Am. Chem. Soc.* **104,** 5266 (1982).
25. Y. Baer and J. Schoenes, *Solid State Commun.* **33,** 885 (1980).
26. T. Thévenin, J. Jové, M. Pagès, and D. Damien, *Solid State Commun.* **40,** 1065 (1981).
27. T. Thévenin, J. Jové, and M. Pagès, *Hyperf. Interact.* **20,** 173 (1984).
28. H. Hashimoto, H. Sakurai, H. Oike, F. Itoh, A. Ochiai, H. Aoki, and T. Suzuki, *J. Phys. Condens. Matter* **10,** 6333 (1998).
29. W. H. Zachariasen, *Acta Crystallogr.* **2,** 291 (1949).
30. E. D. Eastman, L. Brewer, L. A. Bromley, P. W. Gilles, and N. L. Lofgren, *J. Am. Chem. Soc.* **72,** 4019 (1950).
31. G. V. Ellert, V. G. Sevast'yanov, and V. K. Slovyanskikh, *Russ. J. Inorg. Chem. Engl. Transl.* **19,** 1699 (1974).

32. P. D. Shalek, *J. Am. Ceram. Soc.* **46,** 155 (1963).
33. D. E. Eastman and M. Kuznietz, *J. Appl. Phys.* **42,** 1396 (1971).
34. F. A. Wedgewood and M. Kuznietz, *J. Phys. C Solid State Phys.* **5,** 3012 (1972).
35. G. V. Ellert, G. M. Kuz'micheva, A. A. Eliseev, V. K. Slovyanskikh, and S. P. Morozov, *Russ. J. Inorg. Chem. Engl. Transl.* **19,** 1548 (1974).
36. H. P. Beck and W. Dausch, *J. Solid State Chem.* **80,** 32–39 (1989).
37. H. Noël and J. Y. Le Marouille, *J. Solid State Chem.* **52,** 197 (1984).
38. R. C. L. Mooney Slater, *Z. Kristallogr.* **120,** 278 (1964).
39. H. Kohlmann, Ph.D. thesis, University of Saarbrücken, Germany, 1996.
40. A. Daoudi, J. C Levet, M. Potel, and H. Noël, *Mater. Res. Bull.* **31,** 1213 (1996).
41. H. Kohlmann and H. P. Beck, *Z. Anorg. Allg. Chem.* **623,** 785 (1997).
42. I. H. Warren and C. E. Price, *Can. Met. Quart.* **3,** 245 (1964).
43. H. Noël, *J. Inorg. Nucl. Chem.* **42,** 1715 (1980).
44. R. Ferro, *Z. Anorg. Allg. Chem.* **275,** 320 (1954).
45. P. Khodadad, *Bull. Soc. Chim. France* **133** (1960).
46. L. K. Matson, J. W. Moody, and R. C. Himes, *J. Inorg. Nucl. Chem.* **25,** 795 (1963).
47. H. Noël, *Physica B* **130,** 499 (1985).
48. G. V. Ellert, V. G. Sevast'yanov, and V. K. Slovyanskikh, *Russ. J. Inorg. Chem. Engl. Transl.* **20,** 120 (1975).
49. P. T. Moseley, D. Brown, and B. Whittaker, *Acta Crystallogr. Sect. B* **28,** 1816 (1972).
50. P. Khodadad and C. R. Hebd. *Sceances Acad. Sci.* **247,** 1205 (1958).
51. L. Shlyk, R. Troc, and D. Kaczorowski, *J. Magn. Magn. Mater.* **140–144,** 1435 (1995).
52. H. Noël, M. Potel, R. Troc, and L. Shlyk, *J. Solid State Chem.* **126,** 22 (1996).
53. A. Ben Salem, A. Meerschaut, and J. Rouxel, *Compt. Rend. Acad. Sci. Paris Ser. II* **299,** 617 (1984).
54. J. S. Olsen, L. Gerward, U. Benedict, S. Dabos-Seignon, and J. P. Itié, *High Pressure Res.* **2,** 335 (1990).